

## CHARACTERISATION OF ANETHOLE COATED IRON OXIDE NANOPARTICLES AND ASSESSMENT OF ITS BIOLOGICAL ACTIVITY

**Sampathkumar Banupriya, Krishnamoorthy Kavithaa, Palghat Raghunathan Padma and Sundaravadivelu Sumathi\***

Department of Biochemistry, Biotechnology and Bioinformatics Avinashilingam Institute for Home Science and Higher Education for Women, Tamilnadu, India.

**\*Author for Correspondence: Dr. Sundaravadivelu Sumathi**

Department of Biochemistry, Biotechnology and Bioinformatics Avinashilingam Institute for Home Science and Higher Education for Women, Tamilnadu, India.

Article Received on 03/11/2015

Article Revised on 24/11/2015

Article Accepted on 15/12/2015

### ABSTRACT

Synthesis of nanoparticles is carried out with the objective of controlled size, shape and surface coating. There are different forms of nanoparticles such as metallic, non-metallic and oxide. Among these metallic nanoparticles have plenty of applications compared to the bulk materials. The iron oxide nanoparticles were synthesised by co-precipitation method and coated with the compound anethole. Anethole is the compound having anticarcinogenic, antigenotoxic, gastro protective, anti-oxidative, antithrombolytic and vasoactive properties. The coated nanoparticles and uncoated particles were characterised using UV-Visible spectroscopy, Fourier Transform Infrared spectroscopy, X-Ray Diffraction, Energy Dispersive X-ray spectroscopy and Scanning Electron Microscopy analysis to know the absorption peak of the particles, functional group, and nature of the particle and also size of the particles respectively. Further to test its biological activity the antibacterial and antibiofilm activity was assessed using the organisms such as *Escherichia coli*, *Bacillus subtilis*, *Pseudomonas aeruginosa*, *Klebsiella pneumonia* and *Staphylococcus aureus*. The coated particles showed more activity compared to the iron oxide nanoparticles. The cytotoxicity of the nanoparticles was assessed using MTT assay and biocompatibility of the particles was assessed using haemolysis assay.

**KEYWORDS:** Iron oxide nanoparticles, Anethole, Cytotoxicity, Biocompatibility Biofilm, Haemolysis.

### 1. INTRODUCTION

Nanotechnology with its unique physicochemical and biological characteristics concerns the arrangement of material at atomic stage to achieve nanoscale materials.<sup>[1]</sup> Nanotechnology is one of the key technologies in the present century and promises a revolution in the world. In science, nanotechnology deals with the matter at the large scale and it is also used to study the manipulation of matter at the atomic and molecular scale.<sup>[2]</sup> The range of the nanoparticles is between 1 to 100 nm. The nanoparticles are beneficial for human use because of their tiny size and are used in science, technology and medicine.<sup>[3]</sup>

There are different forms of nanoparticles such as metallic, non-metallic and oxide. In industries metal oxide nanoparticles are used to produce products such as catalysts, pigments, food additives, sun screens and cosmetics.<sup>[5]</sup> The special properties of metal nanoparticles have shown interests in the fields such as catalysis, optoelectronics, magnetic, thermal, sensors, fine chemical synthesis, solar energy conversion and medicine.

Nanomedicine is the latest advancement and it is having therapeutic and diagnostic role. Reduction of metal ions in solution is the common method employed to synthesise metal nanoparticles. The chemical and physical methods produce pure and well-defined nanoparticles but they are quite expensive.<sup>[6]</sup> Due to their small size and large surface area, metal nanoparticles, possess cytotoxicity and it also has the ability to generate reactive oxygen species.<sup>[7]</sup> In the past few decades iron oxide nanoparticles have attracted much attention, due to their high surface area easy separation is carried out under magnetic field.<sup>[8]</sup>

The compound anethole occurs naturally and it is mainly present in essential oils as it is an aromatic compound and unsaturated ether. It is sweeter than sugar.<sup>[11]</sup> The nanoparticles are employed as antimicrobial agents. The antibacterial activity of iron oxide nanoparticles have been evaluated against Gram positive and Gram negative bacteria. The organisms do develop resistance against the commonly used antimicrobial agents namely the antibiotics.<sup>[12]</sup> In the present study iron oxide nanoparticles were synthesised by chemical co –

precipitation method and coated with PEG and the compound anethole. The nanoparticles were characterised and it was evaluated by antimicrobial activity and assessed using antibiofilm activity. Haemolysis assay was carried out to evaluate its *in vitro* cytotoxicity and biocompatibility.

## 2. MATERIALS AND METHODS

### 2.1 PREPARATION OF IRON OXIDE NANOPARTICLES

1.35 g of Ferric chloride and 0.99 g of ferrous sulphate heptahydrate was dissolved in 50 ml of double distilled water. 10 ml of 20 M urea solution was added to it. The pH of the solution was adjusted to 8.0 using sodium hydroxide solution and stirred using hot plate magnetic stirrer at 60°C for 3 hours. The colloidal precipitate was separated by external magnet and dried in hot air oven at 65°C overnight. Then the powder was stored for further characterization and evaluation process.

### 2.2 PREPARATION OF ANETHOLE COATED IRON OXIDE NANOPARTICLES

Synthesised particles were coated with the polymer polyethylene glycol. The PEG coated nanoparticles were dissolved in water by stirring for few minutes. Anethole was dissolved in small amount of ethanol and added to it and allowed to stir for 6 to 8 hours continuously till the colour changed to brown. It was centrifuged and washed with distilled water and ethanol. It was finally dried in the hot air oven at 65°C overnight.

### 2.3 CHARACTERISATION OF IRON OXIDE NANOPARTICLES

To determine the tunable optical properties and to exhibit the unique characteristics of the iron oxide nanoparticles the UV-Visible spectrum analysis was carried out. To determine and confirm the crystal structure of iron oxide nanoparticles the XRD studies were employed. FTIR analysis was done to obtain the infra-red spectra of absorption and emission. SEM analysis is used to identify the surface morphology of the sample using NOVA Nano SEM 230.

### 2.4 ANTIBACTERIAL ACTIVITY

Bactericidal activity of iron oxide nanoparticles were tested using the growth inhibition studies against pathogenic microorganisms such as *Escherichia coli*, *Staphylococcus aureus*, *Bacillus subtilis*, *Pseudomonas aeruginosa* and *Klebsiella pneumoniae*. The anethole coated iron oxide nanoparticles and synthesized iron oxide nanoparticles were checked for its antibacterial activity using the disc diffusion method of Pasupuleti *et al.*, (2013)

### 2.5 ANTIMICROBIAL ACTIVITY BY MTT ASSAY

Overnight culture of *Klebsiella pneumoniae* in Muller Hinton Broth was prepared and 95µl of freshly prepared broth was allowed to interact with different concentration of nanoparticles, and kept for incubation at 37°C for 24 hours. 10µl of MTT solution was added to each well and

incubated at 37°C for 4 hours. They were diluted with 100µl of DMSO. Finally the dilutions were read in ELISA reader at 570nm.

### 2.6 ANTIBIOFILM ASSAY

Overnight culture *Staphylococcus aureus* was diluted in the ratio 1:100 in fresh medium and allowed to grow for another hour. 100µl of the diluted strains were added to 96 well titre plate and the different concentrations of nanoparticles were added and incubated at 37°C for 3 days. The growth was monitored every 12 hours at 595nm using ELISA reader. 100µl of 1% crystal violet solution was added and incubated at room temperature for 30 minutes. The wells were washed thoroughly with distilled water and finally incubated with 95% ethanol for 15 minutes and read in spectrophotometer at 595nm.

### 2.7 HAEMOLYSIS ASSAY

The blood was collected in an EDTA tube and it was centrifuged at 4°C 1500 rpm for 5 minutes. The RBC pellets that settled at the bottom were washed three times with PBS and the RBC suspension obtained was diluted with PBS and treated with different concentrations of nanoparticles and they were vortexed gently at 37°C for 60 minutes. The sample incubated with Triton X-100 was considered as positive control (100% lysis) and the sample with PBS buffer as negative control (0% lysis). The Haemolytic activity was analysed by measuring the absorbance of the supernatant at 540nm.

## 3. RESULTS AND DISCUSSION

### 3.1 PREPARATION OF IRON OXIDE NANOPARTICLES

Iron oxide nanoparticles were synthesized by co-precipitation method. The colour changed from yellow to black, confirmed the synthesis of iron oxide nanoparticles. The particles were dried and polyethylene glycol was added as an intermediate for coating the compound anethole. The colour change from black to brown indicated that compound was bound to the synthesised iron oxide nanoparticles.

### 3.2 CHARACTERISATION OF IRON OXIDE NANOPARTICLES

#### 3.2.1 UV-Visible spectroscopy

The results of UV absorption as shown in Fig 1(a) indicated that the iron oxide nanoparticles are having an absorption peak at 380 nm. This indicated that the iron oxide nanoparticles were synthesized. Due to the surface plasmon vibration the peak was observed. Whereas in the case of anethole coated iron oxide nanoparticles whose absorption spectrum is shown in the Fig 1 (b) the peak was observed at 280 nm. This confirms the presence of anethole coated iron oxide nanoparticles.

The absorption peak of anethole ranges between 240 nm to 280 nm was reported by Sinha.<sup>[11]</sup> Narender<sup>[10]</sup> reported that chitosan coated iron oxide nanoparticles showed the absorption range at 365 nm. Similarly the UV visible spectrum of iron oxide nanoparticles showed

absorption at 227 nm indicating the formation of nanosized particles and polydispersity of nanocrystals.<sup>[13]</sup>

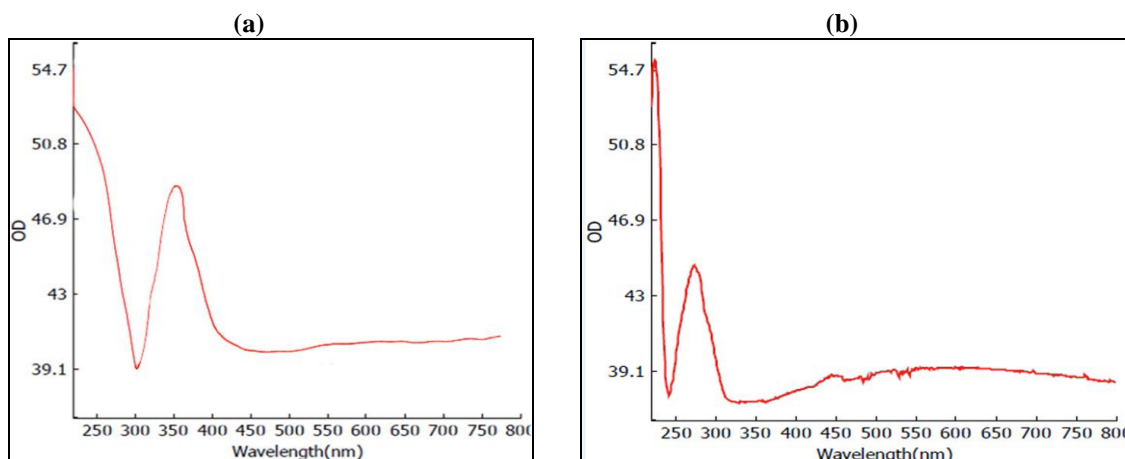


**Fig 1:** UV-Visible spectrum of iron oxide nanoparticles (a) synthesised iron oxide nanoparticles (b) anethole coated iron oxide nanoparticles

### 3.2.2 Fourier Transform Infrared Spectroscopy

The major absorption band spectra of chemically synthesized iron oxide nanoparticles were seen at  $3415\text{ cm}^{-1}$ ,  $2846\text{ cm}^{-1}$ ,  $1023\text{ cm}^{-1}$  and  $890\text{ cm}^{-1}$  as shown in the Fig 2 (a). The absorption peaks at  $3415\text{ cm}^{-1}$  indicated the characteristic bands of hydrogen bonded OH group. The band at  $2846\text{ cm}^{-1}$  showed the presence of carboxylic acid groups. The band at  $1023\text{ cm}^{-1}$  indicated the presence of C-O vibrations associated with the iron oxide nanoparticles. The peak at  $890\text{ cm}^{-1}$  showed the presence of C-O-C stretching vibration of 3, 6 anhydro bridges.

Anethole coated iron oxide nanoparticles showed absorption peaks at  $3410\text{ cm}^{-1}$ ,  $2818\text{ cm}^{-1}$ ,  $1306\text{ cm}^{-1}$  and  $639\text{ cm}^{-1}$ . The results are shown in Fig 3 (b). The peak at

$3410\text{ cm}^{-1}$  indicates the characteristic bands of hydrogen bonded OH group. The band at  $2818\text{ cm}^{-1}$  shows the presence of carboxylic acid groups. The band at  $1306\text{ cm}^{-1}$  indicates the presence of isopropyl group. The peaks at  $639\text{ cm}^{-1}$  indicates the FeO stretching of  $\text{Fe}_2\text{O}_3$  nanoparticles.

Kumar<sup>[14]</sup> reported that the absorption frequency less than  $700\text{ cm}^{-1}$  which indicated the presence of Fe-O vibration of iron oxide nanoparticles. Arokiyaraj<sup>[15]</sup> have reported that the magnetite have absorption peaks at  $566\text{ cm}^{-1}$ ,  $3426\text{ cm}^{-1}$  and  $1635\text{ cm}^{-1}$  indicating the Fe-O stretching, O-H stretching vibration and O-H distorted vibration.

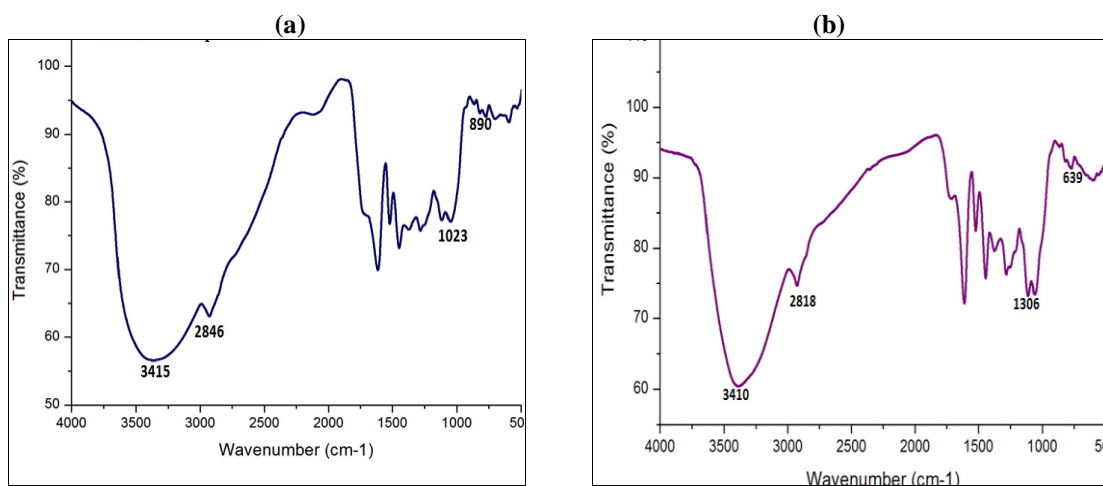


**Fig 2:** FTIR spectrum of iron oxide nanoparticles (a) synthesised iron oxide nanoparticles (b) anethole coated iron oxide nanoparticles

### 3.2.3 Scanning Electron Microscopy

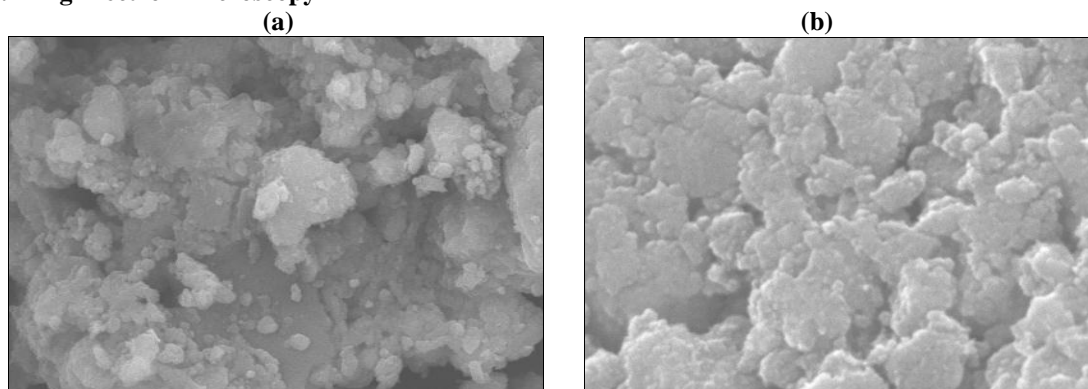


**Fig 3: Scanning Electron Microscopy of iron oxide nanoparticles (a) synthesised iron oxide nanoparticles (b) anethole coated iron oxide nanoparticles**

Under Scanning Electron Microscopy the iron oxide nanoparticles were roughly spherical in shape as shown in Fig 3 (a) whereas the anethole coated iron oxide nanoparticles were clustered together in a nano flower like structure as shown in Fig 3 (b). Khalil<sup>[17]</sup> reported

that synthesized iron oxide nanoparticles were in nanoscale range of  $1\mu\text{m}$ . The HR-SEM images of conventionally prepared  $\text{Mn}_{1-x}\text{Co}_x\text{Fe}_2\text{O}_4$  nanoparticles showed the size ranges from 50-100 nm reported by Amalithi.<sup>[18]</sup>

### 3.2.4 EDX Spectrum

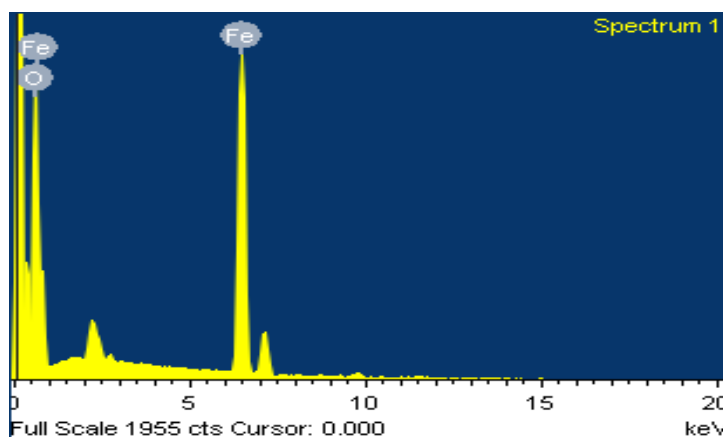


**Fig 4 : EDX spectrum of synthesised iron oxide nanoparticles**

EDX spectrum analysis is used to find the composition of the synthesized nanoparticles. The results of EDX analysis of our present study is shown in Fig 4. The peaks were seen around 0.5, 0.8 and 6.7 keV. It indicated the presence of iron and oxygen and there were no

impurities present in the synthesized iron oxide nanoparticles. Tursunkulov<sup>[16]</sup> reported that sodium oleate coated iron oxide nanoparticles has shown the presence of iron and oxygen components.

### 3.2.5. XRD

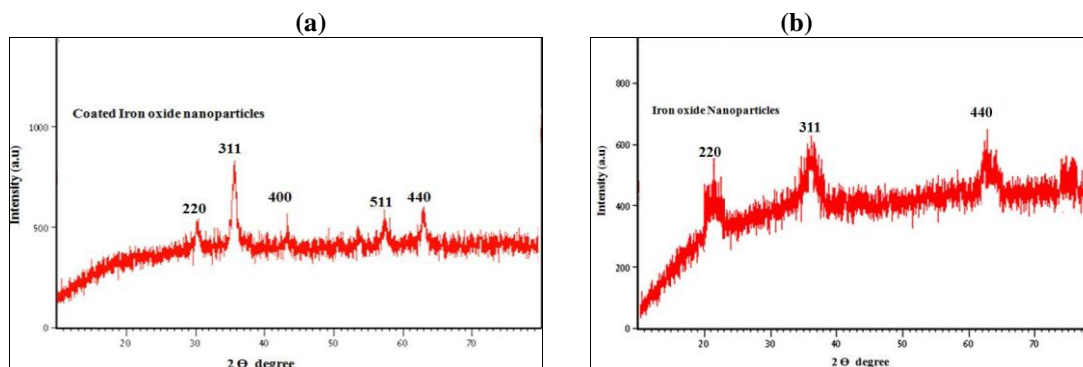


**Fig 5: XRD analysis of iron oxide nanoparticles (a) synthesised iron oxide nanoparticles (b) anethole coated iron oxide nanoparticles**

The crystalline nature of the iron oxide nanoparticles and phase identification were analysed using X-ray Diffraction technique. The peak in the diffractogram indicated that the particles synthesized were crystalline in nature. The powder X-ray diffraction was carried out to identify the nature of the nanoparticles. The results obtained are depicted in the Fig 5. The peak in the figures is indicative of the fact that the synthesized iron oxide nanoparticles and anethole coated iron oxide nanoparticles were crystalline in nature.

Similar studies were reported by other workers. Jafari<sup>[19]</sup> reported that dextran coated iron oxide nanoparticles showed the peaks with  $2\theta$  values of  $35.5^\circ$ ,  $43.0^\circ$ ,  $53.1^\circ$ ,  $57.0^\circ$ ,  $62.5^\circ$  and  $74.2^\circ$  corresponding to the Miller indices (220), (311), (400), (422), (511), (440) and (533). Khalil<sup>[17]</sup> reported that six peaks at  $2\theta$  of  $30.36^\circ$ ,  $35.74^\circ$ ,  $43.52^\circ$ ,  $53.95^\circ$ ,  $57.34^\circ$  and  $63.0^\circ$  which represents the

corresponding indices of (220), (311), (440), (422), (511) and (440) respectively.

### 3.3 Antibacterial activity

The zone of inhibition exhibited by nanoparticles against several bacteria tested is shown in the Fig 6. The zone of inhibition of anethole coated iron oxide nanoparticles for *Pseudomonas aeruginosa* was found to be highest 13mm compared to the iron oxide nanoparticles alone (10mm) and maximum inhibition was for this organism compared to the other strains tested.

Our results are supported by Behera<sup>[XX]</sup> who have reported antibacterial activity of iron oxide nanoparticles. The common mechanism involved in this activity is oxidative stress. Dizaj<sup>[12]</sup> have reported that the antibacterial activity of nanoparticles is due to the inhibition of energy metabolism after internalization of the particles into the microorganisms.

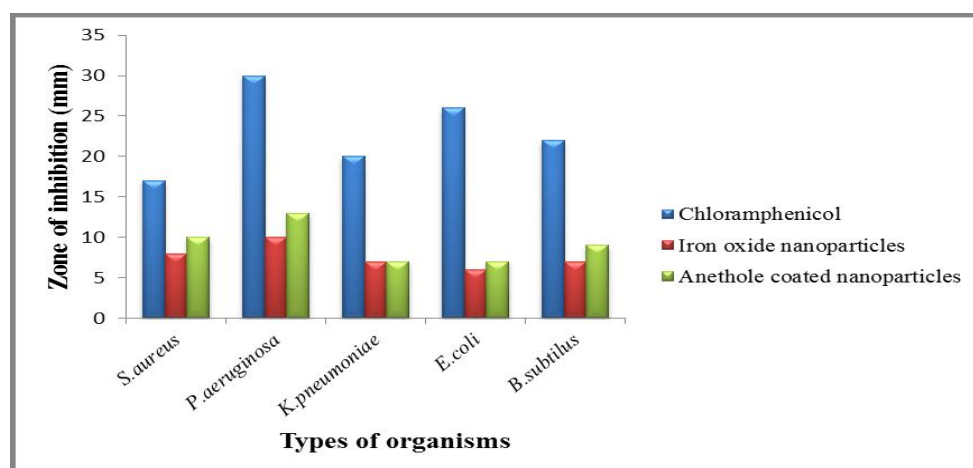


Fig 6: Antibacterial activity of iron oxide and anethole coated iron oxide nanoparticles

### 3.4. Antimicrobial activity by MTT assay

The results of MTT assay as shown in Fig 7 clearly shows that the iron oxide nanoparticles at a concentration of  $10\mu\text{g/ml}$  did not show cytotoxicity. But as the concentration increased the cytotoxicity of iron oxide nanoparticles also increased. The percentage of dead

cells was increased to 61.7% at  $100\mu\text{g/ml}$  and still the percentage can reach up to 100% by increasing the concentration of the coated and uncoated iron oxide nanoparticles. The drug coated nanoparticles were found to possess more cytotoxicity compared to the uncoated iron oxide nanoparticles.

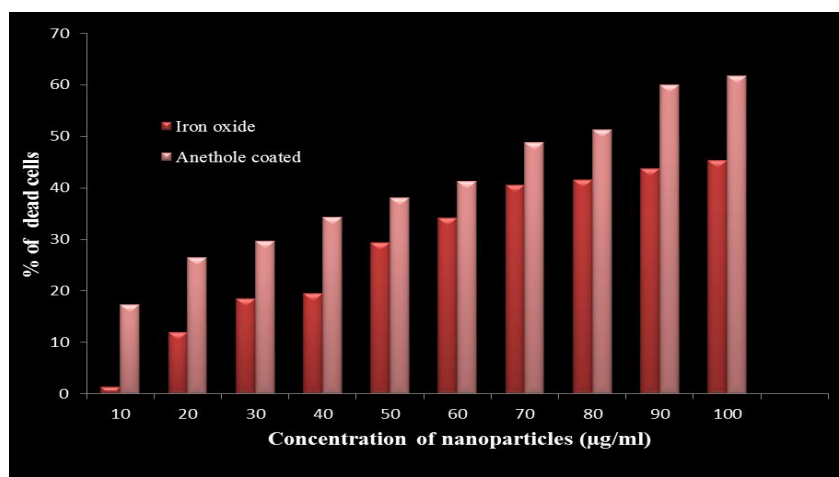


Fig 7 : Antimicrobial activity of iron oxide and anethole coated iron oxide nanoparticles

Abdullah<sup>[21]</sup> have reported that the drug loaded hyaluronan-glutaraldehyde cross-linked nanoparticles inhibits 50% of the cell viability. As the concentration of the nanoparticle increases the cell viability decreases, because the nanoparticles are toxic to the microbial cells.

### 3.5 Antibiofilm activity

Antibiofilm effect of iron oxide and anethole coated iron oxide nanoparticles against biofilm of *Staphylococcus aureus* was studied. Both the nanoparticles were found to exhibit antibiofilm activity in a concentration and dose

dependent manner. But the activity exhibited by anethole coated iron oxide nanoparticles [shown as Fig 8 (b)] was found to be significantly higher compared to iron oxide nanoparticles [as shown in Fig 8 (a)]. At 72 hours anethole coated iron oxide nanoparticles showed nearly 100% inhibition of biofilm formation. Several studies are in accordance with our findings. Namasivayam<sup>[22]</sup> have reported that in biofilm inhibition by silver nanoparticles, it showed 87% inhibition at 72 hours against *Staphylococcus aureus*. These results are in line with our present findings.

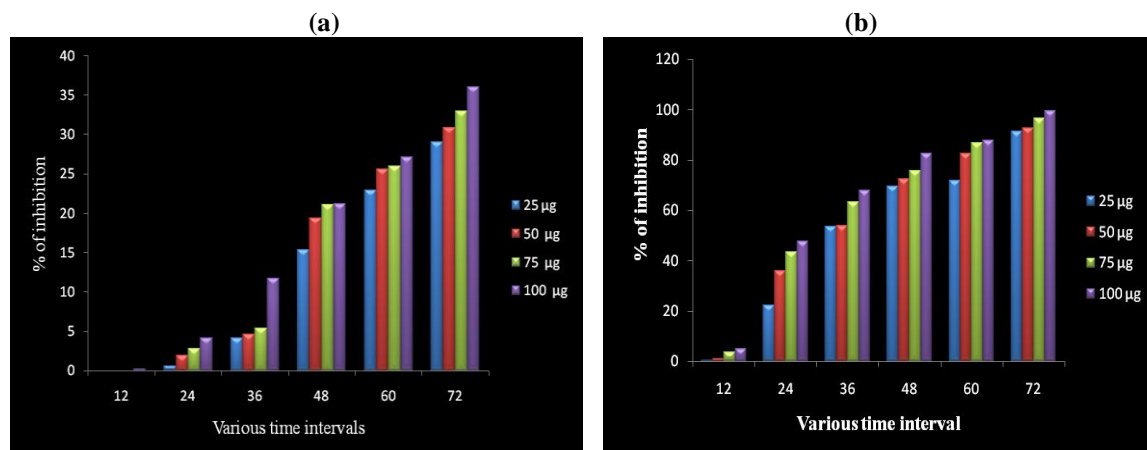


**Fig 8: Antibiofilm activity of iron oxide nanoparticles (a) synthesised iron oxide nanoparticles (b) anethole coated iron oxide nanoparticles**

### 3.6 Haemolysis assay

The haemolysis assay would give additional information about the biocompatibility in the case of *in vivo* applications. For investigating the erythrocyte membrane damaging properties *in vitro* haemolysis assay is followed.

From the Fig 9 it is clear both the particles showed less than 10% of haemolysis in all the concentrations tested. On comparing both the nanoparticles, anethole coated iron oxide nanoparticles showed lesser haemolysis at all

the concentrations and the least was observed at a concentration of 25µg/ml. Several studies have been reported in tune with our findings. Shiny<sup>[23]</sup> reported positive control (Triton X -100) showed lysis of the blood whereas, there was no lysis observed in the supernatant of the nanoparticles treated blood, which was similar to our results. Mocan,<sup>[24]</sup> has reported that the encapsulated nanoparticles showed less than 5% haemolysis and on the other hand 5% lysis was observed as the concentration increased to 1000 µg/ml.

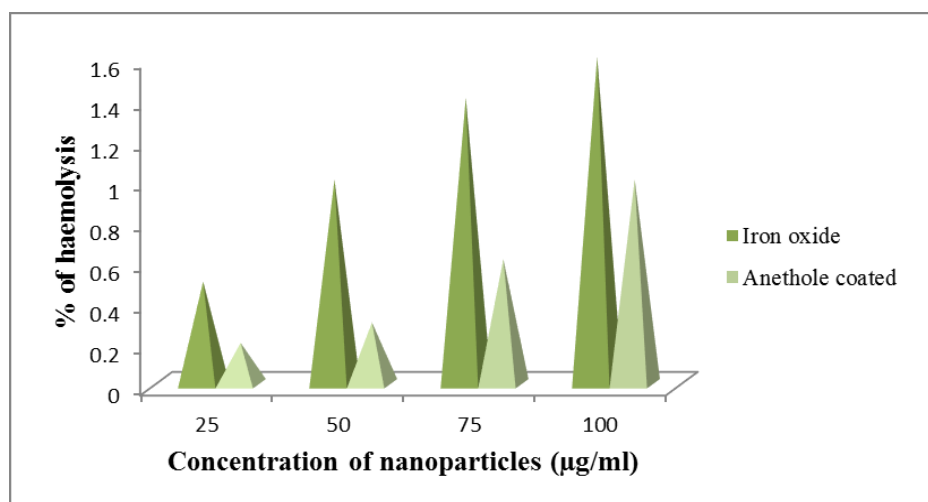


**Fig 9: Haemolysis activity of iron oxide and anethole coated iron oxide nanoparticles**

#### 4. CONCLUSION

The iron oxide nanoparticles were synthesised using cost effective method and it was coated with the compound anethole and their shape and structure were confirmed using characterisation techniques. The cytotoxicity and biocompatibility of the nanoparticles effect were confirmed using MTT and haemolysis assay respectively. It can be further exploited to suit several applications.

#### 6. REFERENCES

1. Vignardi CP, Hasue FM, Sartorio PV, Cardoso CM, Machado ASD, Passos JACR, Santos CA, Thiago N, Watanabe L, Gomes V, Phan NV. Genotoxicity, potential cytotoxicity and cell uptake of titanium dioxide nanoparticles in the marine fish *Trachinotus carolinus*, *Aquatic Toxicol*, 2015; 15: 218-229.
2. Majeed T, Okamura Y, Tanaka T. Biotechnological application of nanoscale engineered bacterial magnetic particles, *J. Mater. Chem*, 2014; 14: 2099-2105.
3. Tonga GY, Moyano FD, Kim CS, Rotello VM. Inorganic nanoparticles for therapeutic delivery: Trials, tribulations and promise, *Colloid and Interface Sci*, 2014; 19: 49-55.
4. Khanehzaei H, Ahmad MB, Shameli K, Ajdari Z. Synthesis and characterization of Cu<sub>2</sub>O core shell nanoparticles prepared in seaweed kappa phycusalvarezii media, *Int. J. Electrochem. Sci*, 2015; 10: 404-413.
5. Ramimoghadam D, Bagheri S, Hamid S, Progress in electrochemical synthesis of magnetic iron oxide nanoparticles, *J. Mag. and Mag. Mat*, 2014; 36: 207-229.
6. Haneefa MM, Jayandran M, Balasubramanian V. Green synthesis of copper nanoparticles using natural reducer and stabilizer and an evaluation of antimicrobial activity, *J. Chem. and Pharm. Res*, 2015; 7: 251-259.
7. Jiang XC, Chen CY, Chen WM, and Yu AB. Role of citric acid in the formation of silver nanoparticles through a synergistic reduction approach, *Int. Nano. Lett*, 2014; 26: 4400-4408.
8. Wang J, Chen Y, Chen B. Pharmacokinetic parameters and tissue distribution of magnetic iron oxide nanoparticles in mice, *Int. J. Nanomed*, 2014; 5: 861-866.
9. Mukherje M. *In vitro* antimicrobial activity of polyacrylamide doped magnetic iron oxide nanoparticles, *Int. J. Materials, Mechanics and Manufacturing*, 2014; 2: 223-235.
10. Narendhar C, Anbarasu S, Divakar S, Gunaseelan R, Sundaram V, Gopu G, Sandesh S. Antimicrobial activity of chitosan coated iron oxide nanoparticles, *Int. J. Chem. Tech. Res*, 2014; 6: 2210-2212.
11. Sinha RK, Shukla S, Jadaun A, Arora V, Biyani N, Jain VK, *In vitro* toxicity assessment of chitosan oligosaccharide coated iron oxide nanoparticles, *Toxicol. Reports*, 2014; 2: 27-39.
12. Dizaj SM, Meenakshi AC, Jafari S, Khezri K, Adibkia K. Antimicrobial activity of carbon based nanoparticles, *Adv. Pharm. Bull*, 2015; 5: 19-23.
13. Rajesh EM, Shamili K, Rajendran R., Elango M, Shankar SRM. Superparamagnetic iron oxide nanoparticles of iron oxide nanoparticles: Synthesis and characterization, *Adv. Sci. Eng. Med*, 2014; 6: 1-5.
14. Kumar SR, Paulpandi, Manivel M, Mangalraj D, Viswanathan C, Kannan S, Ponpandiyam N. An *in vitro* analysis of H1N1 viral inhibition using polymer coated superparamagnetic iron oxide nanoparticles, *Royal Soc. Chem*, 2014; 4: 13409-13418.
15. Arokiyaraj S, Saravanan B, Udaya Prakash NK, Arasu MV, Vijayakumar B Vincent S. Enhanced antibacterial activity of iron oxide magnetic nanoparticles treated with *Argemone mexicana* leaf extract: An *in vitro* study, *Mat. Res. Bulletin*, 2013; 48: 3323-3327.
16. Tursunkulov KN, Mhatre SS, Parikh RY. Biological synthesis of metallic nanoparticles, *Nanomed. Nanotechnol. Biol. Med*, 2013; 6: 257-262.
17. Khalil MI. Co-precipitation in aqueous solution synthesis of magnetite nanoparticles using iron (III) salts as precursors, *Arabian J. Chem*, 2015; 8: 279-284.
18. Amalithi E, Vasile E, Predescu A. Properties of magnetic iron oxides used as materials for wastewater treatment, *J. Phys*, 2015; 32: 345-356.
19. Jafari A, Salouti M, Shayesteh SF, Heidari Z, Boustani K, Nahardani A. Synthesis and characterization of Bombe in superparamagnetic iron oxide nanoparticles as a targeted contrast agent for imaging of breast cancer using MRI, *Nanotechnol*, 2015; 26: 1-11.
20. Behera SS, Patra JK, Pramanik K, Panda N, Thatoi H. Characterization and evaluation of antibacterial activities of chemically synthesized iron oxide nanoparticles, *World J. Nanosci. and Eng*, 2012; 2: 196-200.
21. Abdullah MA, Saba G, Abad A. Cytotoxic effects of drug-loaded hyaluronan-glutaraldehyde cross-linked nanoparticles and the release kinetics modelling, *Int. Adv. Chem*, 2014; 4: 2-9.
22. Namasivayam SK, Preethi M, Bharani RSA, Robin G, Latha B. Biofilm inhibitory effect of silver nanoparticles coated catheter against *staphylococcus aureus* and evaluation of its synergistic effect with antibiotics, *Int. J. Biol. Pharma. Res*, 2013; 3: 259-265.
23. Shiny PJ, Mukherjee A, Chandrasekaran N. Haemocompatibility assessment of synthesised platinum nanoparticles and its implication in biology, *Bioprocess Biosyst. Eng*, 2014; 37: 991-997.
24. Mocan C. Haemolysis as expression of nanoparticles-induced cytotoxicity in red blood cells, *Biotechnology, Mol. Biol. and Nanomed*, 2013; 1: 2-10.